J Mater Sci (2006) 41:5339–5345
DOI 10.1007/s10853-006-0326-y

Characterizations of trimetallic heteronuclear $Bi_{1-x}La_x[Fe(CN)_6]\cdot n(H_2O)$ complexes and their thermal decomposition products

Hiromichi Aono · Nobuyuki Kondo · Haruo Katagishi · Masato Kurihara · Masatomi Sakamoto · Yoshihiko Sadaoka

Received: 15 January 2004 / Accepted: 15 September 2005 / Published online: 6 June 2006

Abstract Heteronuclear $Bi_{1-x}La_x[Fe(CN)_6]\cdot nH_2O$ complexes were synthesized, and their crystal structures and thermal decomposition process were investigated by X-ray diffraction (XRD), thermogravimetry analysis (TGA), Auger electron spectroscopy (AES) with scanning electron microscope (SEM), and transmission electron microscopy (TEM). The crystal system of the complexes was orthorhombic having $n = 4$ for $x = 0$–0.7 and was hexagonal having $n = 5$ for $x = 1.0$. Their mixture was confirmed for $x = 0.8$ and 0.9. The lattice parameters for the orthorhombic increased with increasing the x value for the complexes. The single phase of trimetallic perovskite-type $Bi_{1-x}La_xFeO_3$ was obtained by its thermal decomposition at low temperature. The crystal system was hexagonal for $BiFeO_3$ ($x = 0$) and orthorhombic for $x = 0.1$–1.0. In the case of the decomposed perovskite sample, the lattice parameters decreased with increasing x values for $Bi_{1-x}La_xFeO_3$. The particle size was ca. 30 nm for $Bi_{0.2}La_{0.8}FeO_3$ obtained by thermal decomposition at 500 °C and it grew with an increase in decomposition temperature. For the $Bi_{0.5}La_{0.5}FeO_3$, AES showed that the elemental distributions of Bi, La, and Fe on the surface were very homogeneous for the sample decomposed at 700 °C.

H. Aono (✉) · Y. Sadaoka
Department of Materials Science and Engineering, Faculty of Engineering, Ehime University, Matsuyama 790-8577, Japan
e-mail: haono@eng.ehime-u.ac.jp

N. Kondo
Graduate Program of Human Sensing and Functional Sensor Engineering, Graduate School of Science and Engineering, Yamagata University, Yamagata 990-8560, Japan

H. Katagishi · M. Kurihara · M. Sakamoto
Department of Material and Biological Chemistry, Faculty of Science, Yamagata University, Yamagata 990-8560, Japan

Introduction

Perovskite-type oxides are promising materials for many kinds of applications such as materials for chemical sensors, electrodes for fuel cells, and catalysis [1–5]. $BiFeO_3$ is a perovskite-type phases and the $Bi_{1-x}La_xFeO_3$ solid solution has been reported as ferroelectric properties [6].

In general, polymetallic oxides have been prepared by the conventional solid reaction method. Chemical processing methods such as a sol-gel method are used to obtain fine powders. As a new method, we proposed the thermal decomposition of heteronuclear complexes for the preparation of the di- or tri-metallic oxides. We reported that heterometallic oxides with relatively high specific surface area were formed at low temperatures when heteronuclear hexacyano-complexes were used as the precursors [7–14]. The decomposition of the heteronuclear complexes is a promising method for the preparation of homogeneous mixed oxides on an atomic level [15]. For the di-metallic BiFe-complex, the crystal structure has been investigated for the $Bi[Fe(CN)_6]\cdot nH_2O$ complex [16]. However, trimetallic $Bi_{1-x}La_x[Fe(CN)_6]\cdot nH_2O$ complexes for $Bi_{1-x}La_xFeO_3$ have not been investigated.

In this study, we characterized the $Bi_{1-x}La_x[Fe(CN)_6]\cdot nH_2O$ solid solution system and its decomposition products by X-ray diffraction (XRD), thermogravimetry analysis (TGA), Auger electron spectroscopy (AES) with scanning electron microscopy (SEM), and transmission electron microscopy (TEM).

Experimentals

The heteronuclear complexes, $Bi_{1-x}La_x[Fe(CN)_6]\cdot nH_2O$, were synthesized at room temperature by mixing nitric

acid solutions (2 M/l) of equimolar amounts of $K_3Fe(CN)_6$ and a stoichiometric mixture of $Bi(NO_3)_3 \cdot 5H_2O$ and $La(NO_3)_3 \cdot 6H_2O$ with continuous stirring. The resulting precipitate was collected by suction filtration and then washed with nitric acid solution (2 M/l), water, methanol and diethyl ether, before drying in air at room temperature.

In order to characterize the complexes and the decomposition products, their X-ray diffraction (XRD) patterns using Cu–Kα radiation were recorded (Rint 2000, Rigaku, scanning rate = 2 °/min at 40 kV and 20 mA). The thermal decomposition behavior was examined by TGA analysis, performed at a heating rate of 5 °C/min in air. The heat-treated samples were prepared by holding the complex at various temperatures in ambient air for 1 h. Particle size was evaluated by transmission electron microscopy (TEM, Jeol JEM-100cx) (Bright field image) with selected area diffraction pattern (SADP) measurements at an accelerating voltage of 100 kV (camera length of 600 mm). The surface elemental distribution of Bi, La, and Fe for the decomposed powders were characterized by Auger electron spectroscopy (AES, Perkin-Elmer Phi 650) at a voltage of the incident electron beam of 5 kV. Before AES measurement, the powders were pressed into pellets at a pressure of 1×10^8 Pa and then sputtered with Ar gas for 20 min to remove the surface contaminants before the measurements.

Results and discussion

Figure 1 shows the XRD results for the $Bi_{1-x}La_x[Fe(CN)_6] \cdot nH_2O$ complexes, respectively. For $x = 1.0$ (LaFe-complex), the XRD peak position agreed with that of $La[Fe(CN)_6] \cdot 5H_2O$, which has a hexagonal unit cell (space group: $P6_3/m$) [17, 18]. On the other hand, the XRD peaks showed an orthorhombic unit cell (space group: $CmCm$) having $n = 4$ for $x = 0$–0.7, respectively [19]. For $x = 0.8$–0.9, a mixture of two types of complexes was confirmed by the XRD results. In the case of $x = 0.7$, traces of the hexagonal phase was confirmed in XRD peaks. Figure 2 plots lattice constants for the $Bi_{1-x}La_x[Fe(CN)_6] \cdot nH_2O$ complexes having the orthorhombic (a) structure and the hexagonal (b) unit cell. In the case of orthorhombic complex, all the lattice constants were increased with an increase in x value (La content). This means that the ionic radius of La^{3+} is larger than that of Bi^{3+} in this complex. For this orthorhombic structure, Bi^{3+} and La^{3+} sites in the complex are eight coordination number (8 C.N.) by six nitrogens and two oxygens [15, 20]. In the case of the hexagonal structure, it has been reported that La^{3+} sites in $La[Fe(CN)_6] \cdot nH_2O$ ($x = 1.0$) were coordinated by six nitrogens and three oxygens (9 C.N.)

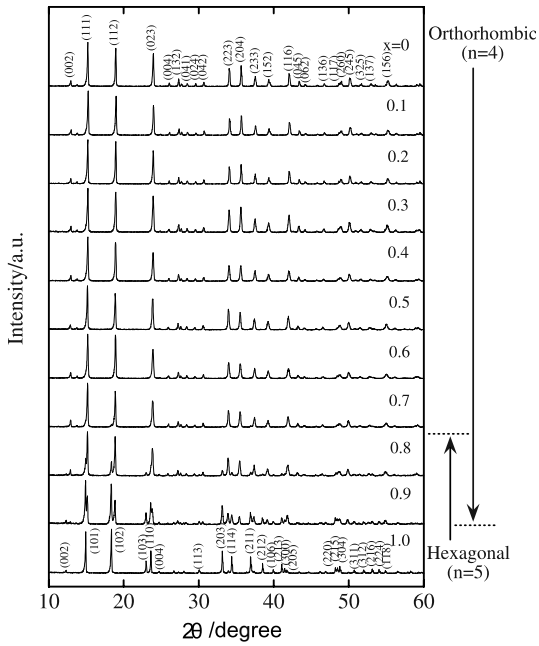

Fig. 1 XRD results of the $Bi_{1-x}La_x[Fe(CN)_6] \cdot nH_2O$ complexes. x-value is shown in the figure

[21]. The lattice constants were hardly changed by a decrease in x value for the hexagonal complex.

Figure 3 shows typical TGA results for the $Bi_{1-x}La_x[Fe(CN)_6] \cdot nH_2O$ complexes, respectively. Dehydration by the loss of water of crystallization started at about 100 °C. A weight loss due to the exothermal decomposition of the ligand (confirmed by DTA) was confirmed at around 300 °C. For $x = 0$ (BiFe-complex), the complex was completely decomposed at around 300 °C. The decomposition temperature increased with an increase in the x value. The weight loss percentages for the dehydration of water and the last plateau range agreed with the theoretical values calculated by assuming the formation of perovskite-type oxides from complexes containing $n = 4$ for $x = 0$, 0.5 and $n = 5$ for $x = 1.0$.

Figures 4 and 5 show the XRD results of the thermal decomposed materials for the $x = 0.5$ and $x = 0.8$ for $Bi_{1-x}La_x[Fe(CN)_6] \cdot 4H_2O$, respectively. In the case of $x = 0.5$ (Fig. 4), the perovskite type phase along with Bi_2O_3 phase and a vitreous phase (estimated from ''halo'') was confirmed in XRD pattern for the samples decomposed below 500 °C. The single phase of the orthorhombic trimetallic perovskite, $Bi_{0.5}La_{0.5}FeO_3$, was obtained at 500 °C. For La-rich $x = 0.8$ sample (Fig. 5), the perovskite phase with ''halo'' was observed in XRD pattern even at 300 °C. The change of peak position for the perovskite phase could not confirm with an increase in decomposition temperature from 300 °C to 1100 °C for all the examined samples.

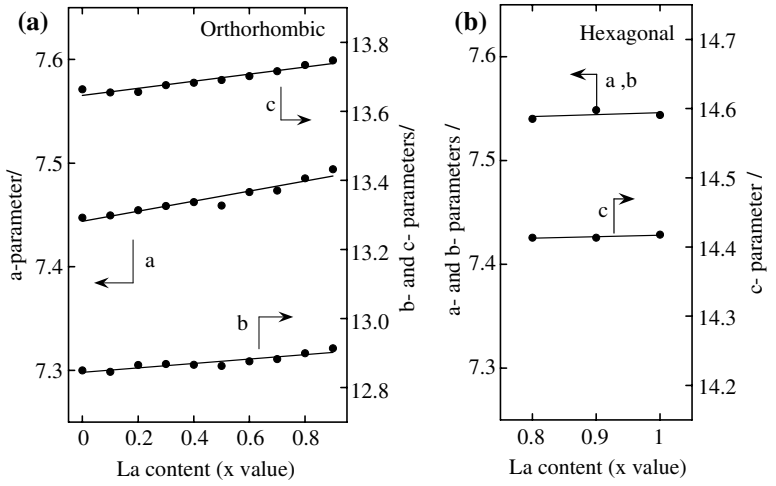

Fig. 2 Lattice parameters of the $Bi_{1-x}La_x[Fe(CN)_6] \cdot nH_2O$ complexes for orthorhombic (**a**) and hexagonal (**b**) structure

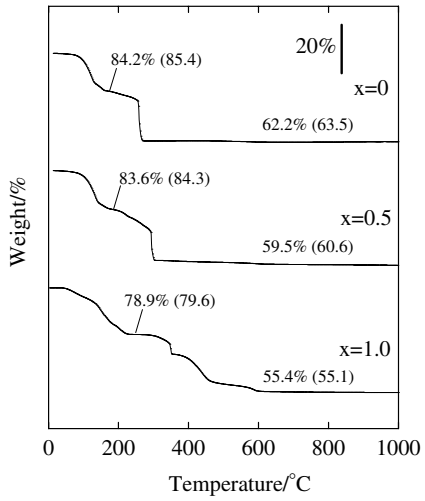

Fig. 3 TGA results for the $Bi_{1-x}La_x[Fe(CN)_6] \cdot nH_2O$ complexes. The weights of the experimental and (theoretical) as $n = 4$ ($x = 0, 0.5$) and $n = 5$ ($x = 1.0$) are shown in the figure

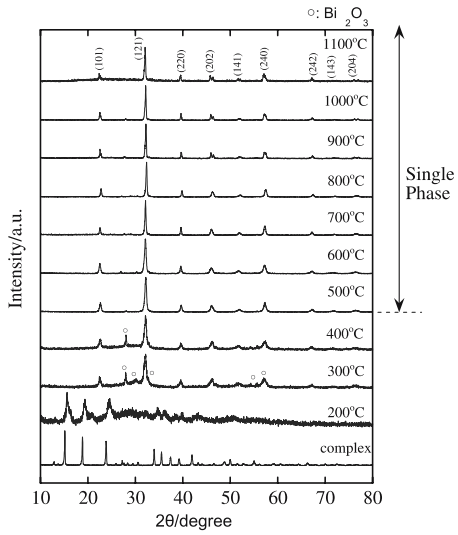

Fig. 4 XRD results of decomposed materials for 1 h at various temperatures for the $Bi_{0.5}La_{0.5}[Fe(CN)_6] \cdot nH_2O$ complex. x-value is shown in the figure

Figure 6 shows XRD results for the $Bi_{1-x}La_xFeO_3$ obtained by the thermal decomposition of the complexes at 800 °C. Single phase was obtained for all the decomposed samples at 800 °C. In the case of $BiFeO_3$ ($x = 0$), XRD peaks showed the formation of hexagonal unit cell (R3-c), which was same unit cell with $LaCoO_3$ [21]. This space group can draw as a trigonal [22]. The unit cell was changed to orthorhombic when La contains in the perovskite even at $x = 0.1$. The change of unit cell from hexagonal to orthorhombic is due to the crystal distortion with the substitution of La^{3+} ion [10]. Figure 7 shows the lattice constants for the $Bi_{1-x}La_xFeO_3$ having the orthorhombic unit cell. The lattice constants linearly decreased with an increase in the x value for the $Bi_{1-x}La_xFeO_3$ and clearly depended on Shannon's ionic radius of the Bi^{3+} ion (0.1170 nm) and the La^{3+} ion (0.116 nm) (8 C.N.) [23]. However, in the case of complex, the opposite result was obtained as shown Fig. 2a, i.e., the lattice constants increased with an increase in La content for the orthorhombic phase. In addition, the lattice constants were almost same value for the hexagonal complex. Shannon has also introduced similar phenomenon for the variable radius Bi^{3+}/La^{3+} ratio for many materials and it explained that the size of Bi^{3+} depends on the degree of the $6s^2$ lone-pair character [23]. Figure 8 shows the phases for the decomposed M = Fe samples. In the case of $BiFeO_3$ ($x = 0$), single phase obtained at 700 °C and it partially decomposed to Bi_2O_3 and Fe_2O_3 when the sample heated above 1000 °C. For $x = 0.2$–0.9, the single phase of the perovskite material obtained at 500 °C. At lower decomposition temperature, the mixed phase of perovskite, Bi_2O_3, and vitreous phase was detected by XRD for $x = 0$–0.7 as shown in Fig. 4. In the case of La-rich samples ($x = 0.8$–1.0), the mixture of

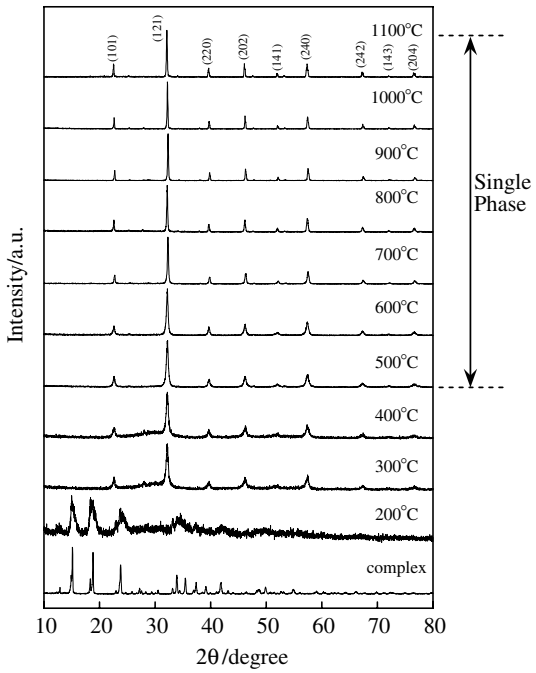

Fig. 5 XRD results of decomposed materials for 1 h at various temperatures for the $Bi_{0.2}La_{0.8}[Fe(CN)_6] \cdot nH_2O$ complex. *x*-value is shown in the figure

perovskite phase and vitreous phase was confirmed for low decomposition temperature even at 300 °C (see Fig. 5). The perovskite type phase would be directly formed by the thermal decomposition of the complex at around 300 °C,

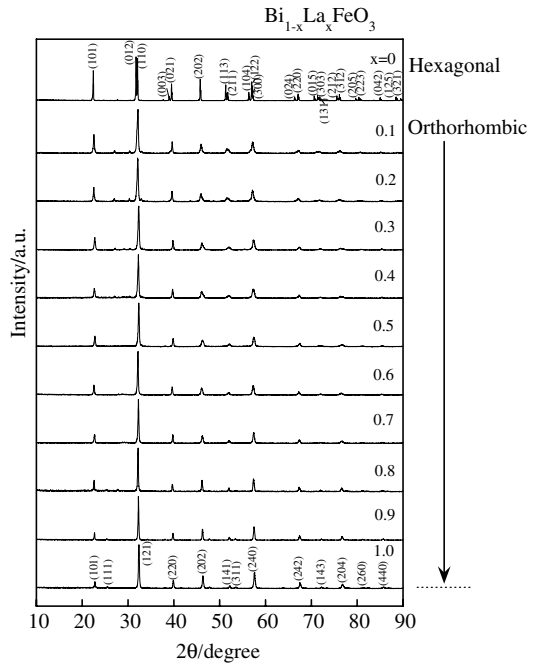

Fig. 6 XRD results of decomposed materials for the $Bi_{1-x}La_x[Fe(CN)_6] \cdot nH_2O$ complexes for 1 h at 800 °C. *x*-value is shown in the figure

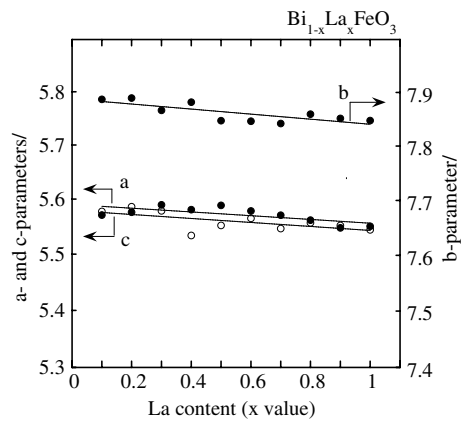

Fig. 7 Lattice parameters of $Bi_{1-x}La_xFeO_3$ obtained by the thermal decomposition of the complexes at 800 °C for 1 h

and then the Bi- and La-ions remaining in other phases such as Bi_2O_3 and vitreous phases reacted to form single perovskite phase at elevated temperature.

Figure 9 shows TEM results for the $Bi_{0.2}La_{0.8}FeO_3$ ($x = 0.8$) particles obtained by the thermal decomposition at 300–700 °C. The particle size for these perovskite samples were around 30 nm at 300–500 °C. Selected area diffraction pattern (SADP) results showed the presence of crystalline diffraction patterns for samples sintered at 300 °C that was in agreement with a calculated pattern for polycrystalline perovskite phase. The particle size increased with an increase in decomposition temperature. Figures 10 and 11 show the SEM-Auger results for the surface of tri-metallic $Bi_{0.5}La_{0.5}FeO_3$ ($x = 0.5$) prepared by using the powder obtained by the complex decomposition

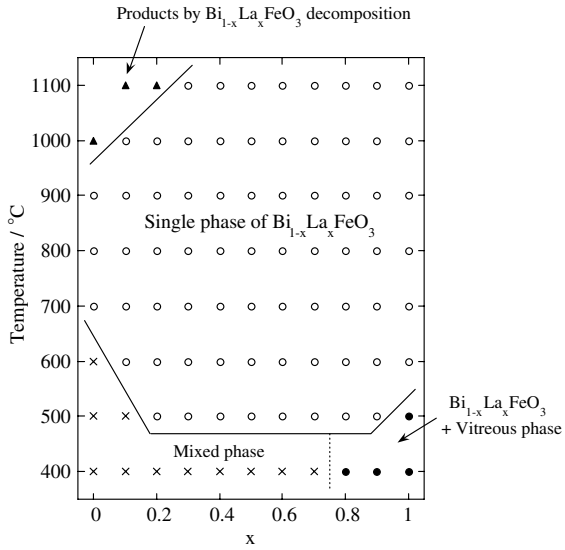

Fig. 8 The phases obtained by thermal decomposition of the $Bi_{1-x}La_x[Fe(CN)_6] \cdot nH_2O$ complexes for 1 h as a function of *x* value and decomposition temperature

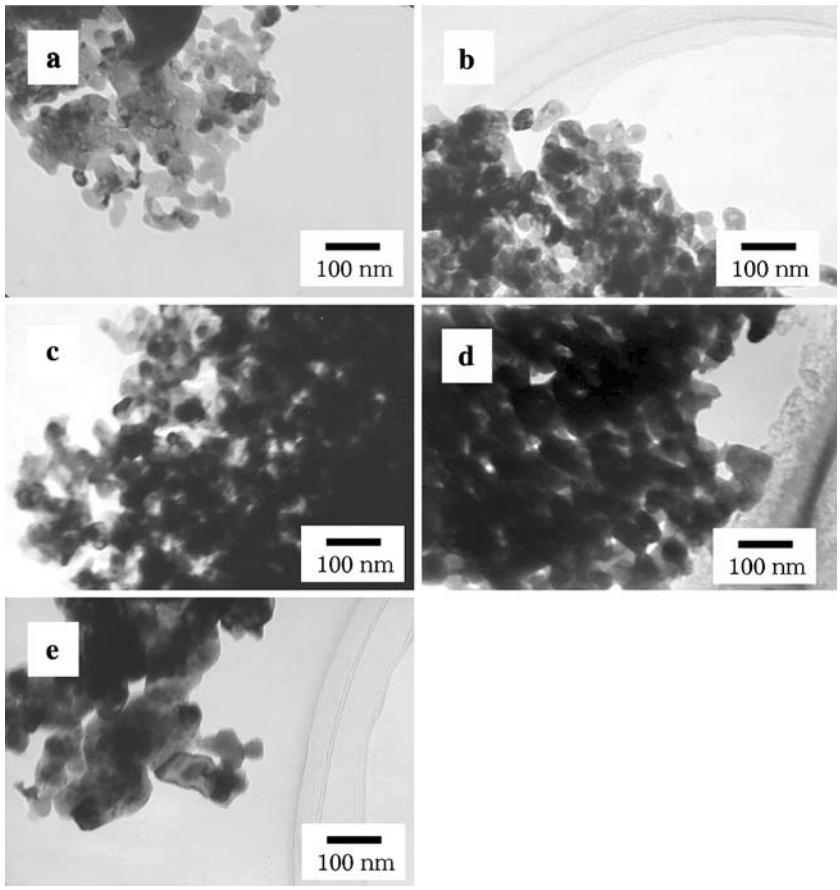

Fig. 9 TEM results for the $Bi_{0.2}La_{0.8}FeO_3$ obtained by the thermal decomposition of the complexes at (**a**) 300 °C, (**b**) 400 °C, (**c**) 500 °C, (**d**) 600 °C, and (**e**) 700 °C for 1 h

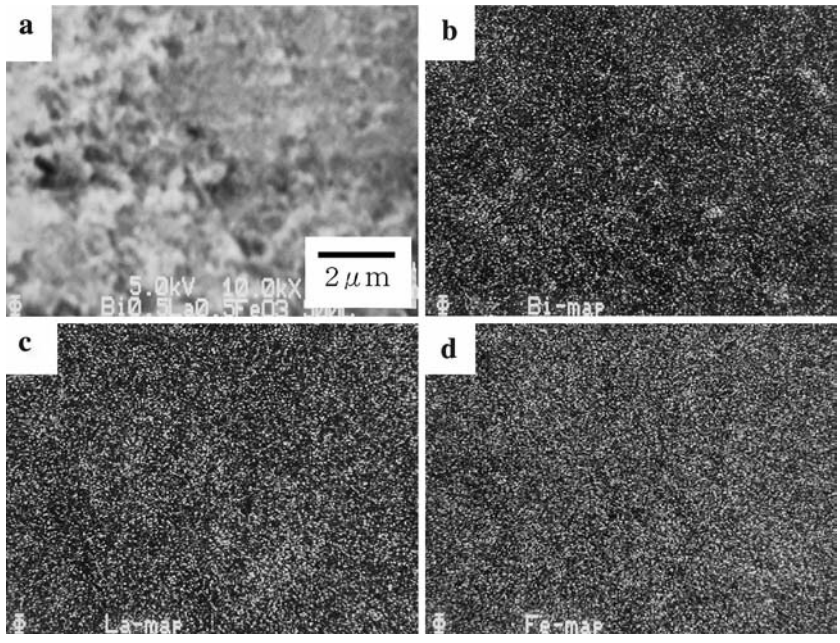

Fig. 10 SEM-Auger results for the $Bi_{0.5}La_{0.5}FeO_3$ obtained by the thermal decomposition of the complex at 500 °C for 1 h. White and black spots in the Auger results represent the high and low concentrations of each analytical element. (**a**) SEM, (**b**) Bi map, (**c**) La map, (**d**) Fe map

at 500 and 700 °C for 1 h, respectively. In the case of the AES measurement, the elemental analysis is very sensitive, because the detectable depth on the surface is around 1 nm. Elemental analyses were operated on the same surface observed by SEM and shown in Fig. 10a and 11a. For the sample decomposed at 500 °C, some insignificant

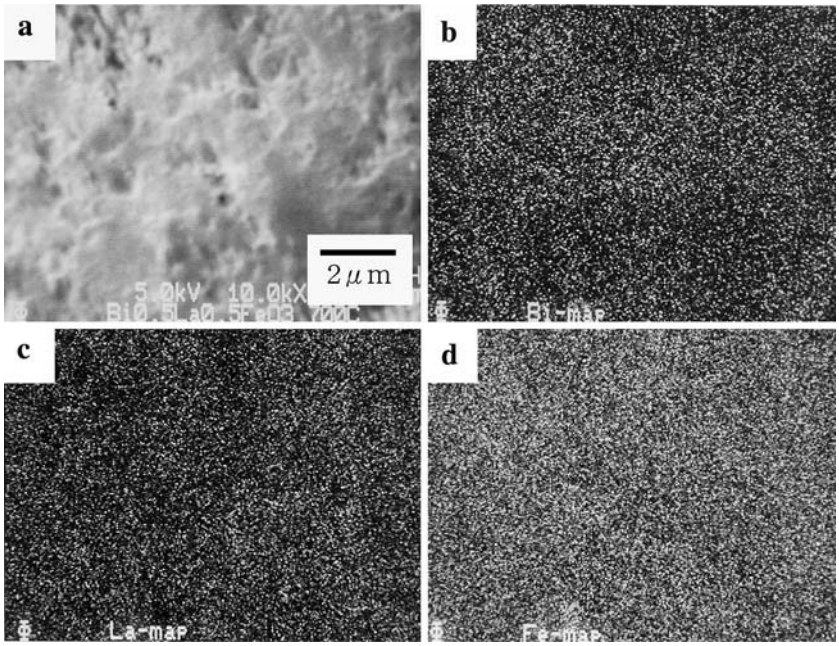

Fig. 11 SEM-Auger results for the $Bi_{0.5}La_{0.5}FeO_3$ obtained by the thermal decomposition of the complex at 700 °C for 1 h. White and black spots in the Auger results represent the high and low concentrations of each analytical element. (**a**) SEM, (**b**) Bi map, (**c**) La map, (**d**) Fe map

heterogeneous white regions were observed in the Bi elemental map. The elemental distribution of La and Fe on the surface was comparatively homogeneous (Fig. 10c, d, respectively). The heterogeneous Bi map for the sample decomposed at 500 °C would be influenced by the formation of Bi_2O_3 phase at lower temperature as shown in Fig. 4. In the case of the sample decomposed at 700 °C, the elemental distribution of Bi, La, and Fe on the surface was highly homogeneous for Fig. 11b, c, d, respectively. Given that inhomogeneities are usually located at grain boundaries and surfaces, it is assumed that the thermal decomposition of the heteronuclear complex is a process suitable to prepare single-phase, homogeneous perovskite-type powders.

Conclusions

The heteronuclear $Bi_{1-x}La_x[Fe(CN)_6]\cdot nH_2O$ complexes were synthesized, and their crystal structures and decomposition process were investigated. Single-phase of tri-metallic $Bi_{1-x}La_xFeO_3$ powders were prepared by the thermal decomposition at 500 °C of the synthesized heteronuclear complexes for $x = 0.2$–0.9. This temperature is the lowest for the single perovskite phase using the thermal decomposition of heteronuclear complex. This method for the preparation of the materials allows the synthesis of high quality of tri-metallic perovskite-type powders, which are homogeneous, single-phase, nano-sized, and free of intragranular pores. These characteristics make these powders very promising for the many applications. In particular, a good processability to form thick-film coatings is expected for these powders, which could be attractive for applications such as magnetic films and chemical sensors.

References

1. Arakawa T, Kurachi H, Shiokawa J (1985) J Mater Sci 4:1207
2. Matsuura Y, Matsushima S, Sakamoto M, Sadaoka Y (1993) J Mater Chem 3:767
3. Traversa E, Matsushima S, Okada G, Sadaoka Y, Sakai Y, Watanabe K (1995) Sensors Actuators B 24/25:661
4. Minh NQ (1993) J Am Ceram Soc 76:563
5. McCarty JG, Wise H (1990) Catal Today 8:231
6. Polomska M, Kaczmarek W, Pajak Z (1974) Phys Status Solidi 23:567
7. Sadaoka Y, Watanabe K, Sakai Y, Sakamoto M (1995) J Alloys Compd 224:194
8. Traversa E, Sakamoto M, Sadaoka Y (1996) J Am Ceram Soc 76:1401
9. Sadaoka Y, Traversa E, Sakamoto M (1996) J Alloys Compd 240:51
10. Sadaoka Y, Traversa E, Sakamoto M (1996) J Mater Chem 6:1355
11. Sakamato M, Nunziante P, Traversa E, Matsushima S, Miwa M, Aono H, Sadaoka Y (1997) J Ceram Soc Jpn 105:963
12. Sadaoka Y, Aono H, Traversa E, Sakamoto M (1998) J Alloys Compounds 278:135
13. Aono H, Kondo N, Sakamoto M, Traversa E, Sadaoka Y (2003) J Eur Ceram Soc 23:1375
14. Aono H, Nakano S, Kondo N, Katagishi H, Sakamoto M, Asato E, Sadaoka Y (2002) Chem Lett 2002(6):568–569
15. Aono H, Kinoshita K, Sadaoka Y, Sakamoto M (1998) J Ceram Soc Jpn 106:958
16. Mullica DF, Perkins HO, Sappenfield EL (1988) Inorg Chim Acta 142:9

17. JCPDS file No.25–1198
18. Mullica DF, Milligan WO, Kouba WT (1979) J Inorg Nucl Chem 41:967
19. Petter W, Gramlich V, Dommann A, Vetsch H, Hulliger F (1990) Inorganica Chimica Acta 170:5
20. Hulliger F, Landolt M, Vetsch H (1976) J Solid State Chem 18:283
21. JCPDS No.251060
22. International Tables for Crystallography (1995) vol. A 19
23. Shannon RD (1976) Acta Crist A32:751